Available online at www.sciencedirect.com
ScienceDirect
Journal of Sound and Vibration 315 (2008) 766–780
JOURNAL OF SOUND AND VIBRATION
www.elsevier.com/locate/jsvi

# Stabilization and utilization of nonlinear phenomena based on bifurcation control for slow dynamics

Hiroshi Yabuno

*Department of Mechanical Engineering, Faculty of Science and Technology, Keio University, 3-14-1 Hiyoshi, Yokohama 223-8522, Japan*

Accepted 5 March 2008
The peer review of this article was organised by the Guest Editor
Available online 5 May 2008

**Abstract**

Mechanical systems may experience undesirable and unexpected behavior and instability due to the effects of nonlinearity of the systems. Many kinds of control methods to decrease or eliminate the effects have been studied. In particular, bifurcation control to stabilize or utilize nonlinear phenomena is currently an active topic in the field of nonlinear dynamics. This article presents some types of bifurcation control methods with the aim of realizing vibration control and motion control for mechanical systems. It is also indicated through every control method that slowly varying components in the dynamics play important roles for the control and the utilizations of nonlinear phenomena. In the first part, we deal with stabilization control methods for nonlinear resonance which is the 1/3-order subharmonic resonance in a nonlinear spring–mass–damper system and the self-excited oscillation (hunting motion) in a railway vehicle wheelset. The second part deals with positive utilizations of nonlinear phenomena by the generation and the modification of bifurcation phenomena. We propose the amplitude control method of the cantilever probe of an atomic force microscope (AFM) by increasing the nonlinearity in the system. Also, the motion control of a two link underactuated manipulator with a free link and an active link is considered by actuating the bifurcations produced under high-frequency excitation. This article is a discussion on the bifurcation control methods presented by the author and co-researchers by focusing on the actuation of the slowly varying components included in the original dynamics.


## 1. Introduction

Mechanical systems generate a great variety of complex nonlinear phenomena [1], which can be often characterized as bifurcation phenomena. The control of the properties of the bifurcation which is called *bifurcation control* makes it possible to suppress the occurrence of nonlinear phenomena and to modify the phenomena to desirable ones. Abed and Fu were among the first to propose the concept of the bifurcation control [2] and in the past two decades, the bifurcation control and the practical applications to real systems have achieved considerable progress. Some fundamental design techniques for bifurcation control are in Ref. [3] and a comprehensive survey of the practical applications to not only mechanical systems but also electrical and biological systems can be found in Ref. [4]. In the case of analyzing local bifurcation behavior near the

*E-mail address:* yabuno@mech.keio.ac.jp

0022-460X/$ - see front matter © 2008 Elsevier Ltd. All rights reserved.
doi:10.1016/j.jsv.2008.03.018

bifurcation point, the first step is to simplify the original governing equations, i.e., to obtain the amplitude equations or averaged equations by the averaging method [5] and the method of multiple scales [6], or other methods and to perform the order reduction of the system by the center manifold theory [5]. The amplitude equation usually expresses the slow time variation of complex amplitude which dominants the steady states and their stability and the reduction corresponds to the extraction of the slow dynamics which determines the essential dynamics. In particular, in the analysis for the stabilization of dynamical systems under high-frequency excitation, the separation of dynamics into slow and fast components [7] and the construction of the subsystem describing the slow dynamics are very important, and by investigating the subsystem the stabilization mechanism is qualitatively clarified [8,9]. Also, some methodologies of bifurcation control based on the dynamics of the subsystem obtained by the above simplification methods are theoretically proposed [10–13].

The purpose of this article is to discuss some bifurcation control for stabilization control and motion control in mechanical systems from the view point of actuating the slowly varying components included in original dynamics. Actuation of the slow dynamics can shift a bifurcation point, eliminate a bifurcation, generate a new bifurcation and modify the nonlinear characteristics of a bifurcation (for example from subcritical bifurcation to supercritical one). As a result, we change the steady states and their stability to avoid undesirable resonance and generate new steady states at desirable positions to perform motion control.

In the first half, we deal with stabilization control of nonlinear phenomena based on bifurcation control. We investigate the control for subharmonic resonance which can be produced in various nonlinear mechanical systems (for example, rotor system [14], buckled beam [15], micro-cantilever [16], and so on). Autoparametric vibration absorber is applied for the stabilization of the 1/3-order subharmonic resonance in a nonlinear spring–mass–damper system [17]. The attachment of the absorber modifies the amplitude equation of the main system and the resonance is suppressed independent of the magnitude of disturbance. Also, we consider the self-excited oscillation (hunting motion) in a railway vehicle wheelset model [18,19]. We design a nonlinear feedback control method for the system reduced on the center manifold in order to avoid the occurrence of the resonance under large disturbance.

In the second half, we discuss positive utilizations of nonlinear phenomena. We propose an amplitude control method for the self-excited micro-cantilever probe of an atomic force microscope (AFM) [20] by artificially increasing the nonlinear viscous damping effect on the system. The utilization of a self-excited cantilever is an idea to keep the resolution of the AFM high accuracy even for biological samples in the liquid environment [21–23]. Then, the small steady-state amplitude of the micro-cantilever is required to avoid the damage to the soft samples by the contact of the beam. For the purpose, an equivalent van der Pol oscillator with small steady-state amplitude is realized by controlling the slow dynamics [24]. Finally, we consider the motion control of a two link underactuated manipulator [25] with an active link and a free link which are actuated and not directly actuated, respectively. The control target is not the amplitude of the motion of the link, but the motion itself. Because the motion is not a slowly varying component, we apply high-frequency excitation so that the time variation of the motion can be regarded as slow. Then, by actuating the slow dynamics, we generate the steady states at desirable positions and change their stability desirably in order to carry out the motion control of the free link without state feedback control [26,27].

This article is a discussion on the nonlinear control methods presented by the author and co-researchers from the point of slowly varying dynamics.

## 2. Slow dynamics

Toward the discussions on bifurcation control based on the slow dynamics in the subsequent sections, we briefly explain the separation of original dynamics into fast and slowly varying components by using a simple example. We examine the dynamics of a spring–mass system with small negative damping whose equation of motion is

$$\frac{\mathrm{d}^2x}{\mathrm{d}t^2} - 2\gamma\omega\frac{\mathrm{d}x}{\mathrm{d}t} + \omega^2 x = 0, \tag{1}$$

where $0<\gamma\ll 1$ and $\gamma=\varepsilon\hat{\gamma}(\hat{\gamma}=O(\varepsilon))$. The exact solution is expressed as

$$x=a_0 e^{\gamma\omega t}\cos(\sqrt{1-\gamma^2}\omega t+\phi_0), \tag{2}$$

where $a_0$ and $\phi_0$ are constants determined by the initial condition. The time history is expressed as Fig. 1 by the fast varying periodic component with frequency near $\omega$ and the slowly varying component corresponding to the time variation of the amplitude, i.e., the envelope of the time history. There are many mechanical systems whose characteristics are determined by the slow dynamics and for such systems, the actuation of the slow dynamics can make it possible to change the principal properties of the dynamics as equilibrium points, their stability, stability of periodic motion, and the magnitude of steady-state amplitude.

Equations governing the slow dynamics correspond to the amplitude equation or averaged equation obtained by asymptotic approaches such as the method of multiple scales, averaging method, and so on [6]. We seek an approximate solution in the form

$$x=x_0+\varepsilon x_1+\cdots. \tag{3}$$

By introducing multiple time scales of $t_0=t$ and $t_1=\varepsilon t$, the first-order approximate solution of the original equation (1) is obtained by the method of multiple scales as follows:

$$x\approx a(t_1)\cos(\omega t_0+\phi_0(t_1)). \tag{4}$$

The slowly varying amplitude $a$ is governed with the following averaged equation or amplitude equation:

$$\frac{da}{dt_1}-\hat{\gamma}\omega a=0 \;\Leftrightarrow\; \frac{da}{dt}-\gamma\omega a=0. \tag{5}$$

Therefore, it is possible to control the stability by changing this equation, i.e., actuating the slow dynamics. While the averaged equations for nonlinear systems are generally much more complex than Eq. (5), they are more suitable to the design of control system than the original equations, because the dependence of the steady states and their stability on the parameters is directly described by the averaged equations. In the following sections, by controlling the slow dynamics, or by generating the slowly varying components, if it is not inherently included in the original dynamics, we accomplish some stabilization control and motion control.

## 3. Stabilization of 1/3-order subharmonic resonance

The pendulum-type vibration absorber is often used as an autoparametric vibration absorber [28] because the pendulum can be autoparametrically excited when the supporting point is vertically excited by the motion of the main system under the case when the frequencies of the main system and the absorber are commensurate [29]. There have been many studies so far since the invention of the autoparametric vibration absorber by Haxton and Barr [30]. Jun et al. [31] theoretically discuss a saturation based absorber which utilizes the mechanism of the autoparametric vibration absorber. Vyas et al. [32,33] theoretically and experimentally investigate the effectiveness of an autoparametric vibration absorber under a wide external

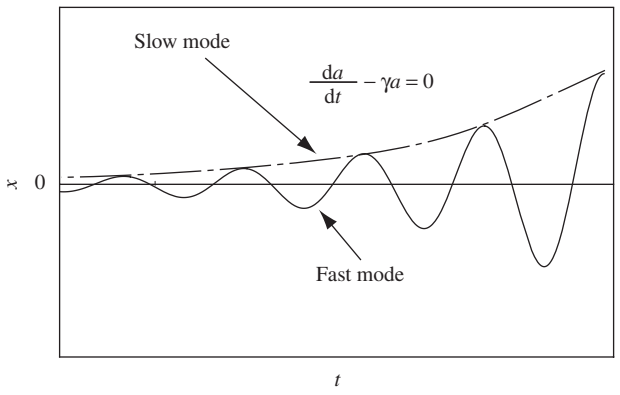


Fig. 1. Fast and slow dynamics of spring-mass system with negative damping.

excitation frequency range using multiple pendulum. The effect of the autoparametric vibration absorber on the parametric resonance is investigated by using the axially excited cantilever beam [34]. We consider the effect of a pendulum-type autoparametric vibration absorber on 1/3-order subharmonic resonance, which is induced depending on the magnitude of disturbance. In contrast with the case under the primary external excitation, the 1/3-order subharmonic frequency component is completely suppressed when the autoparametric vibration absorber is in action [17].

### 3.1. 1/3-order subharmonic resonance

We consider a nonlinear spring–mass–damper system which is sinusoidally excited as shown in Fig. 2(a). The main system can move freely only in $z$-direction. The main system is subjected to quadratic and cubic nonlinear restoring force. The governing equation of motion is derived in the dimensionless form as follows [17]:

$$\ddot{z} + \mu_z \dot{z} + (1 - 2\varepsilon\alpha_{zz} \cos \nu t)z + \alpha_{zz} z^2 + \alpha_{zzz} z^3 = \varepsilon \cos \nu t, \tag{6}$$

where $\alpha_{zz}$ is the proportional constant with respect to the spring elongation squared and $\alpha_{zzz}$ is the proportional constant with respect to the spring elongation cubed. The excitation amplitude $\varepsilon$ is small $(0 < \varepsilon \ll 1)$ and small viscous damping $\mu\dot{z}$ $(\mu_z = O(\varepsilon^2))$ is taken into account. The linear natural frequency is normalized as 1, and the excitation frequency and amplitude are $\nu$ and $\varepsilon$, respectively. It is easy from Eq. (6) to predict that when the excitation frequency of the base $\nu$ is in the neighborhood of triple the natural frequency of the main system, i.e., $\nu = 3 + \sigma(\sigma = O(\varepsilon^2))$, 1/3-order subharmonic resonance is produced. In fact, introducing multiple time scales $t_0 = t$, $t_1 = \varepsilon t$, and $t_2 = \varepsilon^2 t$, and assuming the solution of the main system as follows:

$$z = \varepsilon z_1 + \varepsilon^2 z_2 + \varepsilon^3 z_3, \tag{7}$$

yields an approximate solution as

$$z = a(t) \cos\left\{\frac{\nu}{3} t + \gamma(t)\right\}. \tag{8}$$

Here, we recall that the amplitude and phase, $a$ and $\gamma$, are slowly varied and the slow dynamics are governed by the following averaged equations:

$$\frac{\mathrm{d}a}{\mathrm{d}t} = -\frac{1}{2}\mu_z a - \frac{\varepsilon P_2}{4} a^2 \sin 3\gamma, \tag{9}$$

$$a\frac{\mathrm{d}\gamma}{\mathrm{d}t} = -\left(\frac{\sigma}{3} + \frac{\varepsilon^2 P_1}{2}\right)a - \frac{P_3}{8}a^3 - \frac{\varepsilon P_2}{4} a^2 \cos 3\gamma, \tag{10}$$

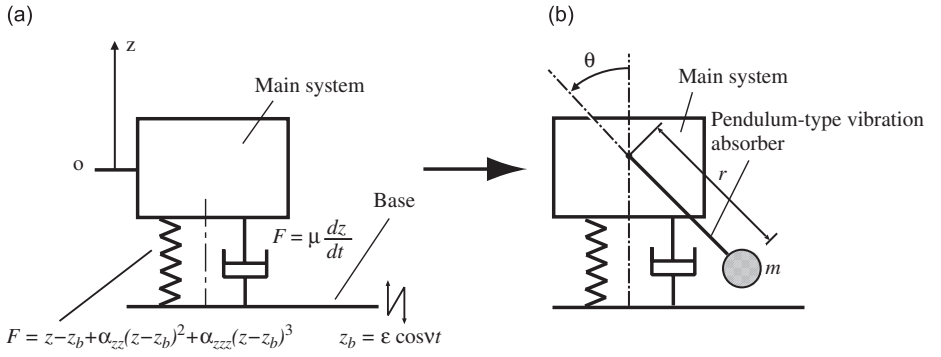


Fig. 2. Nonlinear spring–mass–damper system and application of autoparametric vibration absorber: (a) nonlinear spring–mass–damper system: (b) application of autoparametric vibration absorber.

where $P_1, P_2$, are $P_3$ are constant and expressed as follows:

$$\Lambda = \frac{1}{2(1-\nu^2)},$$
$$P_1 = (2\Lambda - 1)^2 \left\{ \alpha_{zz}^2 \left( \frac{-2}{\nu^2 - 4} + 1 \right) - \frac{3}{2}\alpha_{zzz} \right\},$$
$$P_2 = (2\Lambda - 1) \left\{ -\alpha_{zz}^2 \left( \frac{1}{3} + \frac{2}{\nu(\nu - 2)} \right) - \frac{3}{2}\alpha_{zzz} \right\},$$
$$P_3 = \frac{10}{3}\alpha_{zz}^2 - 3\alpha_{zzz}.$$

From the averaged equations, the frequency response curve is described as Fig. 3(a), where the solid and dashed lines stand for stable and unstable steady-state amplitudes, respectively. The solution of Eqs. (9) and (10) under $\mathrm{d}a/\mathrm{d}t = \mathrm{d}\gamma/\mathrm{d}t = 0$ corresponds to the steady state of the amplitude and the phase, $a_{\mathrm{st}}$ and $\gamma_{\mathrm{st}}$. The stability of the steady state is determined by the eigenvalue of the Jacobian matrix Eqs. (9) and (10) for $a = a_{\mathrm{st}}$ and $\gamma = \gamma_{\mathrm{st}}$. It can be seen from Fig. 3(a) that 1/3-order subharmonic resonance can occur depending on the magnitude of disturbance in the lower excitation frequency range of $\sigma$.

### 3.2. Stabilization by changing averaged equation

The control objective is here to avoid the occurrence of the 1/3-order subharmonic resonance independent of the magnitude of disturbance. By attaching a pendulum-type vibration absorber, we try to stabilize the 1/3-order subharmonic resonance. The equations of motion of the main system and the pendulum are as follows:

$$\ddot{z} + \mu_z \dot{z} + (1 - 2\varepsilon\alpha_{zz}\cos \nu t)z + \alpha_{zz}z^2 + mr(\dot{\theta}^2 - \omega_\theta^2\theta^2) + \alpha_{zzz}z^3 = \varepsilon \cos \nu t, \tag{11}$$

$$\ddot{\theta} + \mu_\theta \dot{\theta} + \left( \omega_\theta^2 + \frac{\ddot{z}}{r} \right)\theta - \frac{1}{6}\omega_\theta^2\theta^3 = 0, \tag{12}$$

where $r$ is the dimensionless length of the pendulum and $\omega_\theta$ is the frequency ratio between the main system and the pendulum. It is necessary that the effect of the absorber changes the averaged equations which govern the slow dynamics and determine the stability of the steady states. For this purpose, we tune the natural frequency of the pendulum as a half the natural frequency of the main system, $\omega_\theta = 1/2 + \rho/2(\rho = O(\varepsilon))$, and increase the number of the resonance terms to produce the secular term, because the averaged equations correspond to the condition not to produce the secular term. We assume an approximate solution as:

$$z = \varepsilon z_1 + \varepsilon^2 z_2 + \varepsilon^3 z_3, \tag{13}$$

$$\theta = \varepsilon\theta_1 + \varepsilon^2\theta_2 + \varepsilon^3\theta_3. \tag{14}$$

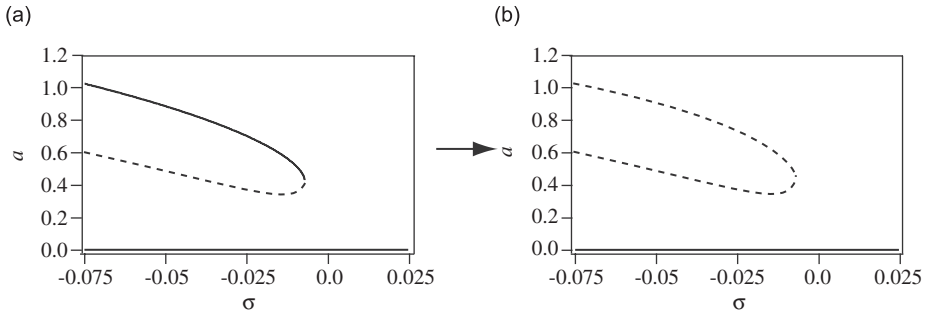


Fig. 3. Change of frequency response curve by autoparametric vibration absorber: (a) absorber is not in action; (b) absorber is in action: $\varepsilon = 0.07$, $m = 0.140$, $r = 4.22$, $\rho = 0.1$, $\alpha_{zz} = -0.65$, $\alpha_{zzz} = 0.359$, $\mu_z = 1.37 \times 10^{-2}$, $\mu_\theta = 3.17 \times 10^{-3}$: —— stable, – – – unstable. (Reprint with permission from H. Yabuno, H. Endo, N. Aoshima, Stabilization of 1/3-order subharmonic resonance using an autoparametric vibration absorber, *Transactions of ASME Journal of Vibration and Acoustics* 121 (1999) 309–315.)

We have an approximate solution of Eqs. (11) and (12) as

$$z = a(t)\cos\left\{\frac{v}{3}t + \gamma(t)\right\} \tag{15}$$

$$\theta = 2b_r(t)\cos\frac{v}{6}t + 2b_i(t)\sin\frac{v}{6}t. \tag{16}$$

By applying the method of multiple scales, we obtain the averaged equations governing the slow dynamics of $a$ and $\gamma$ for the main system and of $b_r$ and $b_i$ for the absorber as follows:

$$\begin{aligned}\frac{\mathrm{d}a}{\mathrm{d}t} = & -\frac{1}{2}\mu_z a - \frac{\varepsilon P_2}{4}a^2\sin 3\gamma \\ & + mr\omega_\theta^2(\rho-2)(b_r^2 - b_i^2)\sin\gamma + 2mr\omega_\theta^2(2-\rho)b_r b_i\cos\gamma,\end{aligned} \tag{17}$$

$$\begin{aligned}a\frac{\mathrm{d}\gamma}{\mathrm{d}t} = & -\left(\frac{\sigma}{3} + \frac{\varepsilon^2 P_1}{2}\right)a - \frac{P_3}{8}a^3 - \frac{\varepsilon P_2}{4}a^2\cos 3\gamma \\ & + mr\omega_\theta^2(\rho-2)(b_r^2 - b_i^2)\cos\gamma - 2mr\omega_\theta^2(2-\rho)b_r b_i\sin\gamma - \frac{P_{12}}{2}(b_r^2 + b_i^2)a,\end{aligned} \tag{18}$$

$$\begin{aligned}\frac{\mathrm{d}b_r}{\mathrm{d}t} = & \left(\frac{\rho}{2} - \frac{\mu_\theta}{2}\right)b_r + \left(\frac{\sigma}{6} + \frac{\varepsilon^2 Q_1}{2\omega_\theta}\right)b_i + \frac{1}{8r\omega_\theta^2}(\rho + 2\omega_\theta)ab_r\sin\gamma \\ & - \frac{1}{8r\omega_\theta^2}(2\omega_\theta + \rho)ab_i\cos\gamma + \frac{Q_3}{2\omega_\theta}(b_r^2 + b_i^2)b_i + \frac{Q_{21}}{8\omega_\theta}a^2 b_i,\end{aligned} \tag{19}$$

$$\begin{aligned}\frac{\mathrm{d}b_i}{\mathrm{d}t} = & \left(\frac{\rho}{2} - \frac{\mu_\theta}{2}\right)b_i - \left(\frac{\sigma}{6} + \frac{\varepsilon^2 Q_1}{2\omega_\theta}\right)b_r - \frac{1}{8r\omega_\theta^2}(2\omega_\theta + \rho)ab_r\cos\gamma \\ & - \frac{1}{8r\omega_\theta^2}(2\omega_\theta + \rho)ab_i\sin\gamma - \frac{Q_3}{2\omega_\theta}(b_r^2 + b_i^2)b_r - \frac{Q_{21}}{8\omega_\theta}a^2 b_r,\end{aligned} \tag{20}$$

where $P_{12}$, $Q_1$, $Q_{21}$, and $Q_3$ are expressed as follows:

$$\begin{aligned}P_{12} &= m\left(\omega_\theta - 3 + \frac{2\omega_\theta}{1+2\omega_\theta}\right), \\ Q_1 &= -\frac{2\Lambda^2 v^4}{r^2(v^2 - 4\omega_\theta^2)}, \\ Q_3 &= \frac{m\omega\theta}{2} - 2m\omega_\theta^2 + \frac{\omega_\theta^2}{2}, \\ Q_{21} &= \frac{-1}{r^2}\left(\frac{1}{1+2\omega_\theta} + \frac{1}{4\omega_\theta^2}\right).\end{aligned} \tag{21}$$

Here, the third and fourth terms in the right-hand side of Eq. (17) and the fourth, fifth, and sixth terms in the right-hand side of Eq. (18) are the effects of the specially frequency tuned pendulum-type vibration absorber and through these terms, the energy transfer between the main system and the absorber is induced. In the case when the absorber is in action, the steady states shown in Fig. 3(b) can be numerically found for the main system. Then, only the steady state of the absorber corresponding to these steady states is stable and trivial. As can be seen from comparison between Figs. 3(a) and (b), the nontrivial steady states of the main system are the same in the cases when the absorber is not in action (the pendulum is mechanically fixed) and in action. However, the stable nontrivial steady state is changed to unstable one and then only the stable steady state is the trivial one. As a result, the 1/3-order subharmonic resonance can be suppressed independent of the magnitude of disturbance. A sufficient condition, such that all the nontrivial steady states are unstable by the effect of the absorber, is derived from the following investigation. The local stability of the steady state

($a = a_{st}$, $\gamma = \gamma_{st}$, $b_r = 0$, $b_i = 0$) is determined from the Jacobian matrix $\mathbf{J}$ of (17)–(20):

$$\mathbf{J} = \begin{bmatrix} J_{11} & J_{12} & 0 & 0 \\ J_{21} & J_{22} & 0 & 0 \\ 0 & 0 & J_{33} & J_{34} \\ 0 & 0 & J_{43} & J_{44} \end{bmatrix}, \tag{22}$$

where

$$\begin{aligned}
J_{11} &= -\frac{\mu_z}{2} - \frac{\varepsilon P_2}{2} a_{st} \sin 3\gamma_{st}, \quad J_{12} = -\frac{\varepsilon P_2}{4} a_{st}^2 \cos 3\gamma_{st}, \\
J_{21} &= -\frac{\sigma}{3a_{st}} - \frac{\varepsilon^2 P_1}{2a_{st}} - \frac{3P_3}{8} a_{st} - \frac{\varepsilon P_2}{2} \cos 3\gamma_{st}, \quad J_{22} = \frac{\varepsilon P_2}{4} a_{st} \sin 3\gamma_{st}, \\
J_{33} &= \frac{\rho}{2} - \frac{\mu_\theta}{2} + \frac{1}{8r\omega_\theta^2}(2\omega_\theta + \rho) a_{st} \sin \gamma_{st}, \\
J_{34} &= \frac{\sigma}{6} + \frac{\varepsilon^2 Q_1}{2\omega_\theta} + \frac{Q_{21}}{8\omega_\theta} a_{st}^2 - \frac{1}{8r\omega_\theta^2}(2\omega_\theta + \rho) a_{st} \cos \gamma_{st} \\
J_{43} &= -\frac{\sigma}{6} - \frac{\varepsilon^2 Q_1}{2\omega_\theta} - \frac{Q_{21}}{8\omega_\theta} a_{st}^2 - \frac{1}{8r\omega_\theta^2}(2\omega_\theta + \rho) a_{st} \cos \gamma_{st}, \\
J_{44} &= \frac{\rho}{2} - \frac{\mu_\theta}{2} - \frac{1}{8r\omega_\theta^2}(2\omega_\theta + \rho) a_{st} \sin \gamma_{st}.
\end{aligned}$$

Here, $a_{st}$ and $\gamma_{st}$ are those obtained from Eqs. (9) and (10) in the case when the absorber is not in action. Also, the $2 \times 2$ upper left matrix of the Jacobian matrix $\mathbf{J}$ is the same as the Jacobian matrix of Eqs. (9) and (10) for $a = a_{st}$ and $\gamma = \gamma_{st}$. Then, the stability of the nontrivial steady state of the main system, in the case when the absorber is in action, is determined by the eigen value of the $2 \times 2$ lower right matrix:

$$\mathbf{J}' = \begin{bmatrix} J_{33} & J_{34} \\ J_{43} & J_{44} \end{bmatrix}. \tag{23}$$

Therefore, a sufficient condition such that matrix $\mathbf{J}'$ has an unstable eigenvalue is $J_{33} + J_{44} = \rho - \mu_\theta > 0$. This method is based on the modification of the bifurcation characteristics in the slow dynamics and can be classified into bifurcation control.

## 4. Nonlinear control for hunting motion of railway vehicle wheelset

### 4.1. Hunting motion of railway vehicle wheelset

Railway vehicle wheelset experiences the problem of hunting above a critical running speed [35] due to circulatory [36] contact force between the wheels and the rails. The two-degrees-of-freedom model with respect to lateral and yawing motions, $y$ and $\psi$, is shown in Fig. 4. The wheelset is suspended with springs from the truck. The wheelset generally has the tread angle $\gamma_e$ as shown in this figure to make the running performance on a curved rail smoother. On the other hand, this tread angle makes the running performance on the straight rail worse owing to the following reason. We consider the situation in which the wheelset is moving in the positive $y$-direction under disturbance. The peripheral speed of the part of the left wheel in contact with the rail is higher than that of the right one. Also, because the left and right wheels have the same angular velocity, slips between the wheels and rails occur and a special contact force, that is, the so called creep force, is produced on the surface of the wheels. The equations of motion are as follows [19]:

$$m\ddot{y} = -\frac{2\kappa_y}{v}\dot{y} - ky + 2\kappa_y\psi \tag{24}$$

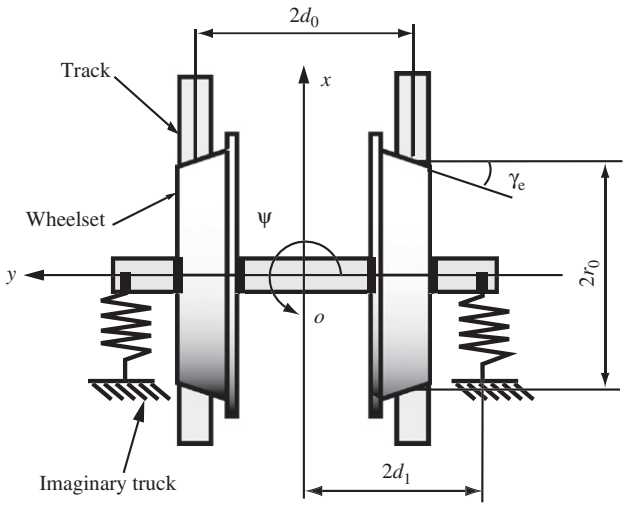


Fig. 4. Two-degrees-of-freedom model of railway vehicle wheelset.

$$I\ddot{\psi} = -\frac{2d_0^2\kappa_x}{v}\dot{\psi} - \frac{2d_0\kappa_x\gamma_e}{r_0}y - M\psi, \tag{25}$$

where $m$, $I$, $\kappa_x$, $\kappa_y$, $k_y$, $k$, $M$, $2d$, $r_0$, and $v$ are the mass of wheelset, the moment of inertia, the longitudinal creep coefficient, the lateral creep coefficient, stiffness in the $y$-direction, a proportional constant of restoring moment, the gauge, the radius of the wheel at the contact point to the rail, and running speed, respectively.

In a high-speed run, it is known that the contact force causes a self-excited oscillation called hunting motion. This occurs because the contact force appears as nonconservative or circulatory forces, which is the third term in the right-hand side of Eq. (24) and the second term in the right-hand side of Eq. (25). From the root loci of the equations of motion with respect to $v$, the critical speed $v_{cr}$, above which the hunting motion is produced, is obtained in the linear sense and the critical speed corresponds to the stability boundary in the case of a small disturbance. Under a large disturbance, the hunting motion can be produced even below the critical speed, because at the critical speed, subcritical Hopf bifurcation [37] occurs. Therefore, the equations of motion, Eqs. (24) and (25), can be rewritten to the following equations which include cubic nonlinear terms:

$$\begin{aligned} m\ddot{y} = & -\frac{2\kappa_y}{v}\dot{y} - ky + 2\kappa_y\psi \\ & + k_{yyy}y^3 + k_{yy\psi}y^2\psi + k_{y\psi\psi}y\psi^2 + k_{\psi\psi\psi}\psi^3 \end{aligned} \tag{26}$$

$$\begin{aligned} I\ddot{\psi} = & -\frac{2d_0^2\kappa_x}{v}\dot{\psi} - \frac{2d_0\kappa_x\gamma_e}{r_0}y - M\psi \\ & + M_{yyy}y^3 + M_{yy\psi}y^2\psi + M_{y\psi\psi}y\psi^2 + M_{\psi\psi\psi}\psi^3. \end{aligned} \tag{27}$$

Furthermore, these equations are nondimensionalized as

$$\dot{\mathbf{x}} = \begin{bmatrix} 0 & 1 & 0 & 0 \\ -c_1 & -c_2 & c_3 & 0 \\ 0 & 0 & 0 & 1 \\ -c_5 & 0 & -1 & -c_4 \end{bmatrix}\mathbf{x} + \begin{bmatrix} 0 \\ c_1\varepsilon\dot{y}^* + c_6y^{*3} + c_7y^{*2}\psi + c_8y^*\psi^2 + c_9\psi^3 \\ 0 \\ c_4\varepsilon\dot{y}^* + c_{10}y^{*3} + c_{11}y^{*2}\psi + c_{12}y^*\psi^2 + c_{13}\psi^3 \end{bmatrix},$$
$$\mathbf{x} = [y^* \;\; \dot{y}^* \;\; \psi \;\; \dot{\psi}]^{\mathrm{T}}, \tag{28}$$

where dimensionless parameters $c_6 \cdots c_{13}$ are assumed as nonlinear effects of contact force. The dimensionless running speed $v^*$ is assumed to be in the neighborhood of the critical speed $v_{cr}^*$: $v^* - v_{cr}^* = \varepsilon(|\varepsilon| \ll 1)$. Slow

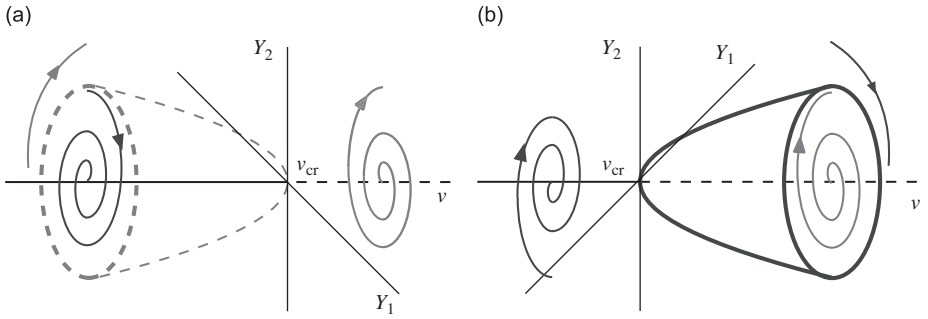


Fig. 5. Slow dynamics on center manifold.

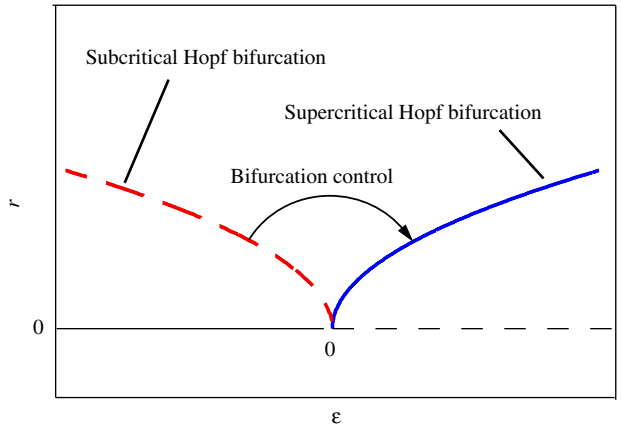


Fig. 6. Radius of limit cycle and nonlinear control (—— stable, – – – unstable).

dynamics, which is extracted from the original dynamics by the center manifold theory, is described on the plane as Fig. 5(a); the original forth-order dynamics of Eq. (28) is reduced to second-order slow dynamics. The distance of the locus from the origne on the plane is expressed from normal form theory [5] as

$$\dot{r} = \alpha_1 \varepsilon r + \alpha_3 r^3, \tag{29}$$

where $\alpha_1 > 0$ and $\alpha_3 > 0$. The magnitude of the unstable limit cycle produced through the subcritical Hopf bifurcation corresponds to the dashed branch in Fig. 6. Therefore, the hunting motion can be produced under a large disturbance even if the running speed is below the critical speed $c_{cr}$. In the next section, we propose a nonlinear control method to stabilize the hunting motion below the critical speed independent of the magnitude of disturbance.

### 4.2. Design of nonlinear feedback gain on center manifold

By applying nonlinear control force proportional to $y$ cubed to the wheelset in the $y$-direction, we change the subcritical Hopf bifurcation to a supercritical Hopf one. The nonlinear feedback gain is designed on the center manifold to bend the bifurcation branch to the right as the solid branch in Fig. 6. The effect of the nonlinear feedback appears in the coefficient of the second term in Eq. (30) as

$$\dot{r} = \alpha_1 \varepsilon r + (\alpha_3 - \alpha_{3-\mathrm{cont}}) r^3, \tag{30}$$

where $\alpha_{3-\mathrm{cont}}$ is the nonlinear feedback gain on the center manifold transformed from the original nonlinear feedback gain $k_{\mathrm{non}}$ under control force in $y$ direction, $F_{\mathrm{cy}} = -K_{\mathrm{non}} y^3$, that is added to Eq. (24). In order to change the subcritical Hopf to the supercritical one, we determine $K_{\mathrm{non}}$ so that $\alpha_{3-\mathrm{cont}}$ is larger than $\alpha_3$. Then,

there is no unstable limit cycle below the critical speed and the hunting motion cannot occur below the critical speed, independent of the magnitude of disturbance.

We have introduced stabilization control methods for nonlinear phenomena, in Sections 3 and 4. In the latter half of this paper, we consider useful applications of nonlinear phenomena for amplitude control and motion control. Also in these cases, slow dynamics play important roles in their applications.

## 5. Amplitude control of AFM cantilever probe

### 5.1. Principle of atomic force microscopy and control objective

AFM has been applied widely as a powerful tool for nanoscale imaging in surface science and biological science [38]. Frequency modulation atomic force microscopy (FM-AFM) is a method of observing the profile of the surface by detecting the equivalent natural frequency of the cantilever probe (Fig. 7) [39] depending on the distance between the tip of the probe and the surface and by observing frequency modulation while scanning the surface. There are two difficulties for the application to the imaging of living biological samples. The first one comes from the use in a liquid environment. The high damping causes poor-quality factor for the oscillation of the cantilever. The other difficulty is based on the need to keep the molecules biologically active. It requires sensing with as low a contact force as possible. To overcome the first difficulty, the frequency modulation (FM) detection by self-excited oscillation in the cantilever beam has been proposed [23] because the response frequency of the self-excited oscillation is self-tuned and always the natural frequency of the system even if it is changed; this characteristic of the self-excited oscillation has been also utilized to keep resonant state for realizing machines with high productivity and low energy consumption [40]. The purpose of this study is to devise a method of overcoming the second difficulty. We propose an amplitude control method for the self-excited cantilever probe [24].

### 5.2. Van der Pol type self-excited cantilever probe

The self-excited cantilever probe has been realized by applying positive linear velocity feedback control. In this case, as predicted by the characteristic of the self-excited oscillation, the amplitude of the self-excited beam is determined by the magnitude of nonlinearity of the environment, for example, the cubic damping effect. To make the steady-state amplitude sufficiently small, we apply an additional nonlinear damping via nonlinear feedback. As a result, we design the dynamics equivalent to a van der Pol oscillator in the cantilever. We consider an analytical model of a cantilever beam with a piezo actuator as shown in Fig. 8 [41] and apply voltage to the piezo actuator on the basis of a nonlinear feedback equation such as

$$V_a = K_2 \left.\frac{\partial v}{\partial t}\right|_{s=l} - K_3 v^2 \left|_{s=l} \left.\frac{\partial v}{\partial t}\right|_{s=l}, \right. \tag{31}$$

where the first term is the positive velocity feedback for production of self-excited oscillation. The second term is the equivalent nonlinear viscous damping for realizing the dynamics of the van der Pol oscillator in the micro-cantilever and for carrying out amplitude control. In Fig. 8, the coordinate is set along the cantilever's

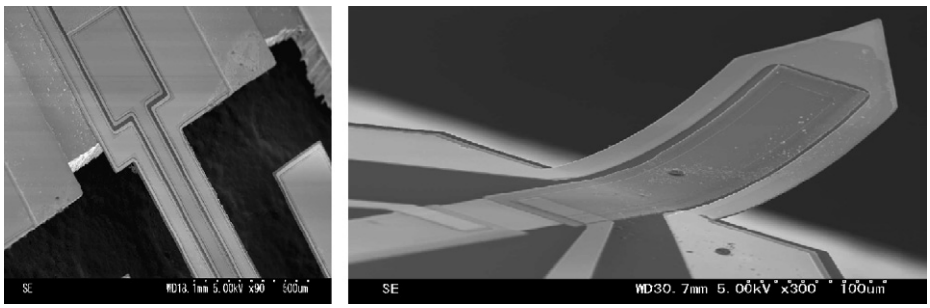


Fig. 7. Micro-cantilever.

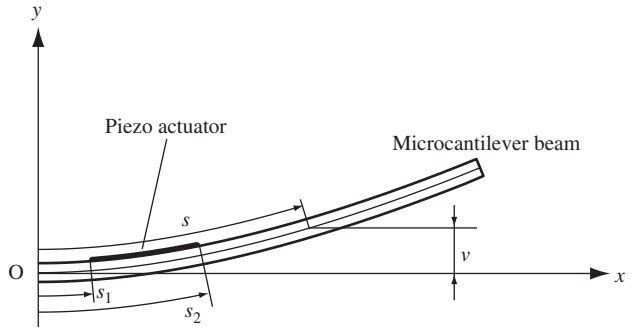


Fig. 8. Analytical model of micro-cantilever.

elastic axis as $s$. The transverse deflection with respect to the deformed axis at $s$ is $v(s,t)$. The cantilever is assumed to behave as an Euler–Bernoulli beam. The dimensionless equation of motion and the associated boundary conditions are

$$\ddot{v}^* + (\mu_{\text{lin}} + \mu_{\text{non}} v^{*2})\dot{v}^* + v^{*\prime\prime\prime\prime} = \{k_{\text{lin}}\dot{v}^*|_{s^*=1} - k_{\text{non}} v^{*2}|_{s^*=1}\dot{v}^*|_{s^*=1}\}[h(s^* - s_1^*) - h(s^* - s_2^*)]'', \tag{32}$$

$$v^{*\prime\prime\prime}|_{s^*=1} = v^{*\prime\prime}|_{s^*=1} = v^{*\prime}|_{s^*=0} = v^*|_{s^*=0} = 0. \tag{33}$$

The derivatives with respect to $t^*$ and $s^*$ are denoted, respectively, as $\dot{()}$ and $()'$. The second term in the left-hand side of Eq. (32), $(\mu_{\text{lin}} + \mu_{\text{non}} v^{*2})\dot{v}^*$ is the damping effect in the environment. The right-hand side in Eq. (32) expresses the effects of the feedback to make characteristics of van der Pol oscillator; $k_{\text{lin}}$ and $k_{\text{non}}$ are linear and nonlinear feedback gains, respectively.

### 5.3. Slow dynamics and amplitude control

We scale the parameters as $\mu_{\text{lin}} = \varepsilon^2\hat{\mu}_{\text{lin}}$, and $k_{\text{lin}} = \varepsilon^2\hat{k}_{\text{lin}}$, where the order of parameters with the symbol of $\hat{()}$ is $O(1)$. We apply the method of multiple scales. Third-order uniform expansion of the solution is determined letting $v^*$ in the form

$$v^* = \varepsilon v_1 + \varepsilon^3 v_3 + \cdots = \frac{\varepsilon}{2} a(t_2) e^{i\phi(t_2)} e^{i\omega t_0} \Phi_1(s) + \varepsilon^3 e^{i\omega t_0}\Phi_3(s,t_2) + \text{CC} + \cdots, \tag{34}$$

where $t_0 = t$ is the first time scale to express the time variation of the periodic component and $t_2 = \varepsilon^2 t$ is the stretched time scale to express the time variation of the complex amplitude due to the nonlinearity. CC denotes the complex conjugate of the preceding terms, and $\omega$ and $\Phi_1(s)$ are the linear first natural frequency and the fist mode shape. Equating like powers of $\varepsilon$ yields

$$D_0^2 v_1 + v_1^{\prime\prime\prime\prime} = 0, \tag{35}$$

$$v_1^{\prime\prime\prime}|_{s^*=1} = v_1^{\prime\prime}|_{s^*=1} = v_1^{\prime}|_{s^*=0} = v_1|_{s^*=0} = 0, \tag{36}$$

$$D_0^2 v_3 + v_3^{\prime\prime\prime\prime} = -2D_2 D_0 v_1 - (\hat{\mu}_{\text{lin}} + \mu_{\text{non}} v_1^2) D_0 v_1 + \{\hat{k}_{\text{lin}} - k_{\text{non}} v_1^2|_{s^*=1}\} D_0 v_1|_{s^*=1}[h(s^* - s_1^*) - h(s^* - s_2^*)]'', \tag{37}$$

$$v_3^{\prime\prime\prime}|_{s^*=1} = v_3^{\prime\prime}|_{s^*=1} = v_3^{\prime}|_{s^*=0} = v_3|_{s^*=0} = 0, \tag{38}$$

where $D_0$ and $D_2$ are derivative with respect to $t_0$ and $t_2$, respectively. The slow time variation of the amplitude $a$ is governed by the following averaged equation which is the solvability condition

of $\Phi_3$ [24]:

$$\frac{da}{dt} + \left(\frac{\mu_{\text{lin}}}{2} - \beta_1 k_{\text{lin}}\right)a + \frac{1}{4}(\beta_2\mu_{\text{non}} + \beta_3 k_{\text{non}})a^3 = 0, \tag{39}$$

where $\beta_1, \beta_2$, and $\beta_3$ are constant functions of $\Phi_1$. This amplitude equation is equivalent to that of van der Pol oscillator. The steady-state amplitude is

$$a_{\text{st}} = \sqrt{\frac{4\beta_1 k_{\text{lin}} - 2\mu_{\text{lin}}}{\beta_2\mu_{\text{non}} + \beta_3 k_{\text{non}}}}. \tag{40}$$

When the positive velocity feedback gain satisfies $k_{\text{lin}} < \mu_{\text{lin}}/(2\beta_1)$, the self-excited oscillation occurs. Higher nonlinear feedback gain of $k_{\text{non}}$ accomplishes the self-excited oscillation with smaller steady-state amplitude to avoid the contact with the sample.

## 6. Motion control of underactuated manipulator by bifurcation control under high-frequency excitation

Finally, we propose the motion control of an underactuated manipulator shown in Fig. 9(a). This two link system has no actuator at the second joint, and the number of degrees-of-freedom is greater than the number of actuators. Such manipulators are generally called underactuated manipulators (a comprehensive list of references can be found in Ref. [25]). From the practical point of view, the investigation into the motion control is very useful for overcoming actuator failure due to unexpected accidents in space environment. Our control objective is to swing up the free link to the upright position and stabilize it at this state. Different from conventional studies on underactuated manipulators, we consider the situation where a free joint lacks not only an actuator but also a sensor. Because state feedback control is not utilized in this situation, we try to actuate slow dynamics similar to the previous three control methods. However, while the amplitude control is accomplished by focusing on the slowness of the time variation of amplitude in the previous problems, the control target in the underactuated manipulator is not the amplitude but the state of the angle. In order to use the approach based on the actuation of the slow dynamics as well as the previous problems, the time variation of the state of the angle has to be regarded as slow. To this end, we apply a periodic excitation with high-frequency which is much higher than the natural frequency of the free link [27].

### 6.1. Bifurcation control of free link

We set the position of the first link, that is, the active link, as

$$\theta_1 = a_e \cos\omega t + \theta_{1\text{off}}. \tag{41}$$

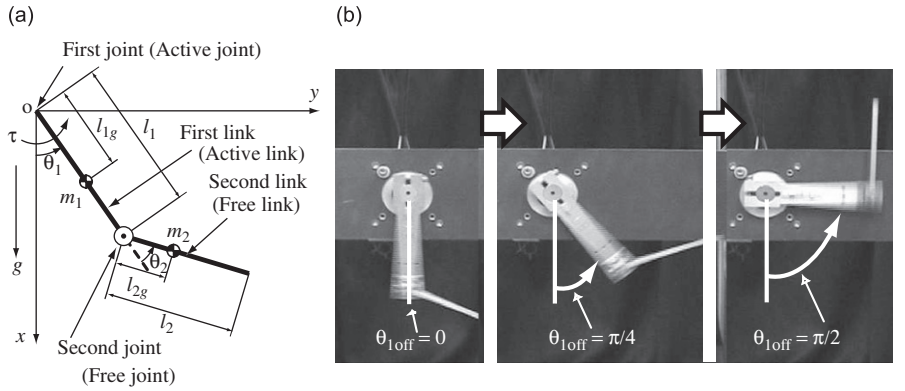


Fig. 9. Underactuated manipulator: (a) analytical model of underactuated manipulator; (b) demonstration of swing-up by bifurcation control: $m_1 = 1.1 \times 10^{-1}$kg, $m_2 = 2.14 \times 10^{-2}$kg, $l_1 = 1.02 \times 10^{-1}$m, $l_2 = 1.00 \times 10^{-1}$m, $l_{1g} = 5.70 \times 10^{-2}$m, $l_{2g} = 1.65 \times 10^{-2}$m, $I_2 = 1.74 \times 10^{-5}$kg m$^2$, $\omega/(2\pi) = 45$Hz. (Reprint with permission from H. Yabuno, H. Matsuda, N. Aoshima, Reachable and stabilizable area of an underactuated manipulator, *IEEE/ASME Transactions on Mechatronics* 10 (2005) 397–403. ©E2005 IEEE.)

The first term is for giving high-frequency excitation, and the second term expresses the configuration of the first link with respect to the direction of the gravitational force. For example, when $\theta_{1\text{off}}$ is 0, the second joint is approximately excited in the horizontal direction. When $\theta_{1\text{off}}$ is $\pi/2$, the second joint is approximately excited in the vertical direction. In this state, the free link has the dynamics similar to Kapitza pendulum [42]. It is theoretically shown that by changing $\theta_{1\text{off}}$ from 0 to $\pi/2$, the second link can be swung up as the experimental result in Fig. 9(b).

Under this excitation, the dimensionless equation of motion is expressed as

$$\ddot{\theta}_2 + \mu\dot{\theta}_2 - a_e c\cos t^* \cos\theta_2 + a_e^2 c \sin\theta_2 + \sigma\sin(a_e\cos t^* + \theta_{1\text{off}} + \theta_2) = a_e\cos t^*, \tag{42}$$

where $t^*$ is the dimensionless time, $\mu$ expresses the dimensionless damping ratio, and the other dimensionless parameters are as follows:

$$c = \frac{m_2 l_1 l_{2g}}{I_2 + m_2 l_{2g}^2}, \quad \sigma = \frac{m_2 l_{2g} g}{(I_2 + m_2 l_{2g}^2)\omega^2}.$$

The parameters, $m_2$, $l_2$, $l_{2g}$, and $I_2$, denote the mass and length of the free link, the distance between the free joint and the center of gravity, and the mass moment of inertia about the center of the free link, respectively. The parameter $l_1$ denotes the length of the active link. The parameter $\sigma$ is proportional to the inverse of the excitation frequency $\omega$ squared and small $\sigma$ means high-frequency excitation. We introduce multiple time scales as $t_0 = t^*$, $t_1 = \varepsilon t^*$, and $t_2 = \varepsilon^2 t^*$, and assume the uniform expansion of the solution as $\theta_2 = \theta_{20} + \varepsilon\theta_{21} + \varepsilon^2\theta_{22}$. Then, by applying the method of multiple scales, we can extract the averaged equation governing the slow dynamics as follows [26]:

$$\ddot{\theta}_2 + \mu\dot{\theta}_2 + \sigma\sin(\theta_{1\text{off}} + \theta_2) - \frac{c^2 a_e^2}{2}\sin\theta_2\cos\theta_2 \approx 0. \tag{43}$$

Because the equation is autonomous, we carry out bifurcation analysis.

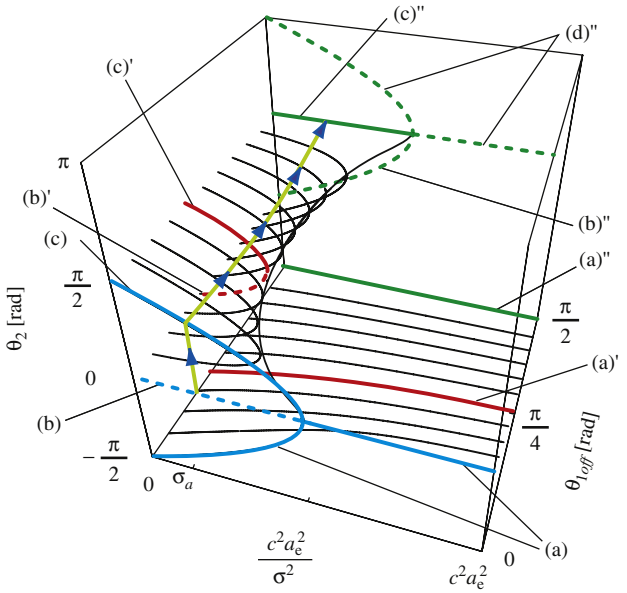


Fig. 10. Equilibrium space of free link (The combination of branches of (a), (b), and (c) is supercritical pitchfork bifurcation. The combination of branches of (a)′, (b)′, and (c)′ is perturbed supercritical pitchfork bifurcation. The combination of branches of (c)″and (d)″is subcritical pitchfork bifurcation. The stable branches of (c), (c)′ and (c)″are smoothly connected from $\theta_{1\text{off}} = 0$ to $\pi/2$. The free link is swing up along the line with arrow on the surface formed by these stable branches.) (Reprint with permission from H. Yabuno, K. Goto, N. Aoshima, Swing-up and stabilization of an underactuated manipulator without state feedback control, *IEEE Transactions on Robotics and Automation* 20 (2004) 359–365.©E2004 IEEE.)

Fig. 10 [26] shows the equilibrium space of the free link with respect to the parameters $\sigma$ and $\theta_{1\mathrm{off}}$; solid and dashed lines denote stable and unstable equilibrium states, respectively. The supercritical and subcritical pitchfork bifurcations are produced in the cases of $\theta_{1\mathrm{off}} = 0$ (combination of branches of (a), (b), and (c)) and $\theta_{1\mathrm{off}} = \pi/2$ (combination of branches of (c)″ and (d)″), respectively. Also, in the case of $0 < \theta_{1\mathrm{off}} < \pi/2$, branches formed by the combination of perturbed supercritical and subcritical pitchfork bifurcations exist as the red lines. We can see in Fig. 10 a perturbed supercritical pitchfork bifurcation which is the combination of branches of (a)′, (b)′, and (c)′. The stable branches of (c), (c)′, and (c)″ are smoothly connected from $\theta_{1\mathrm{off}} = 0$ to $\pi/2$. Therefore, in the high-frequency excitation range (for example $\sigma = \sigma_a$), the stable steady state of the free link is continuously changed from the downward position to the upright position with increase of $\theta_{1\mathrm{off}}$. Then, we carry out the swinging-up of the free link from the downward position along the line with arrow and the stabilization at the upright position.

## 7. Summary

We have introduced vibration and motion control methods for some mechanical systems. As mechanical systems become lighter, faster, and more flexible, various nonlinear phenomena can be easily produced. The essential characteristics such as stability and bifurcation are usually described by slowly varying components included in the original dynamics. Therefore, it is effective to actuate the slow dynamics not only for suppressing the occurrence of nonlinear phenomena but also for positively utilizing the properties of nonlinear phenomena. Also, regarding the final topic of an underactuated manipulator, the positive utilization of nonlinearity inherently existing in mechanical systems is expected to realize high-performance mechanical systems.

## Acknowledgments

The author would like to express his thanks to Drs. T. Kobayashi and M. Kuroda, researchers in Advanced Industrial Science and Technology (AIST) for offering the pictures of micro-cantilever and their insightful comments for cantilever probe of AFM and to Mr. H. H. Jo, a graduate student in University of Tsukuba for his assistance. This work was supported by Grants-in-Aid for Scientific Research of Japanese Ministry of Education, Culture, Sports, Science and Technology No. 19560225.

## References

[1] E. Jackson, *Perspectives of Nonlinear Dynamics 1 and 2*, Cambridge University Press, Cambridge, 1991.
[2] E. Abed, J. Fu, Local feedback stabilization an bifurcation control, *Systems and Control Letters* 7 (1986) 11–17.
[3] G. Chen, J. Moiola, H. Wang, Bifurcation control: theories, methods, and applications, *International Journal of Bifurcation and Chaos* 10 (2000) 511–548.
[4] G. Chen, D. Hill, X. Yu, *Bifurcation Control*, Springer, Berlin, 2003.
[5] J. Guckenheimer, P.J. Holmes, *Nonlinear Oscillations, Dynamical Systems, and Vector Fields*, Springer, New York, 1983.
[6] A.H. Nayfeh, *Introduction to Perturbation Techniques*, Wiley, New York, 1981.
[7] D. Tchherniak, J. Thomsen, Slow effects of fast harmonic excitation for elastic structures, *Nonlinear Dynamics* 17 (1998) 227–246.
[8] J.J. Thomsen, *Vibrations and Stability, Advanced Theory, Analysis, and Tools*, Springer, Berlin, 2003.
[9] I.I. Blekhman, *Vibrational Mechanics*, World Scientific, Singapore, 2000.
[10] W. Steiner, A. Steindl, H. Troger, Center manifold approach to the control of a tethered satellite system, *Applied Mathematics and Computation* 70 (1995) 315–327.
[11] P. Yu, Bifurcation dynamics in control system, in: G. Chen, D. Hill, X. Yu (Eds.), *Bifurcation Control*, Springer, Berlin, 2003, pp. 99–126.
[12] Z. Wu, P. Yu, A method for stability and bifurcation control, *IEEE Transactions on Automatic Control* 51 (2006) 1019–1023.
[13] H. Yabuno, Bifurcation control of parametrically excited Duffing system by a combined linear-plus-nonlinear feedback control, *Nonlinear Dynamics* 12 (1997) 263–274.
[14] T. Inoue, Y. Ishida, Chaotic vibration and internal resonance phenomena in rotor systems, *Transactions of the ASME Journal of Vibration and Acoustics* 128 (2006) 156–169.
[15] S.A. Emam, A.H. Nayfeh, Nonlinear response of buckled beams to subharmonic-resonance excitations, *Nonlinear Dynamics* 35 (2004) 105–122.

[16] E.M. Abdel-Rahman, A.H. Nayfeh, Contact force identification using the subharmonic resonance of a contact-mode atomic force microscopy, *Nanotechnology* 16 (2005) 199–207.
[17] H. Yabuno, Y. Endo, N. Aoshima, Stabilization of 1/3-order subharmonic resonance using an autoparametric vibration absorber, *Transactions of the ASME Journal of Vibration and Acoustics* 121 (1999) 309–315.
[18] H. Yabuno, T. Okamoto, N. Aoshima, Effect of lateral linear stiffness on nonlinear characteristics of hunting motion of a railway wheelset, *Nonlinear Dynamics* 37 (2002) 555–568.
[19] H. Yabuno, T. Okamoto, N. Aoshima, Stabilization control for the hunting motion of a railway wheelset, *Vehicle System Dynamics* 35 (2001) 41–55.
[20] G. Binning, C.E. Quate, C. Gerber, Atomic force microscope, *Physical Review Letters* 56 (1986) 930–933.
[21] T. Albrecht, P. Grutter, D. Horne, D. Ruger, Frequency modulation detection using high-Q cantilever for enhanced force microscope sensitivity, *Journal of Applied Physics* 69 (1991) 668–673.
[22] A. Humphris, J. Tamayo, M. Miles, Active quality factor control in liquids for force spectroscopy, *Langmuir* 16 (2000) 7891–7894.
[23] T. Okajima, H. Sekiguchi, H. Arakawa, A. Ikai, Self-oscillation technique of AFM in liquids, *Applied Surface Science* 210 (2003) 68–72.
[24] H. Yabuno, H. Kaneko, M. Kuroda, T. Kobayashi, Van der Pol type self-excited micro-cantilever probe of atomic force microscopy, Nonlinear Dynamics, in press.
[25] H. Arai, K. Tanie, N. Shiroma, Nonholonomic control of a three-dof planar underactuated manipulator, *IEEE Transactions on Robotics and Automation* 14 (1998) 681–695.
[26] H. Yabuno, K. Goto, N. Aoshima, Swing-up and stabilization of an underactuated manipulator without state feedback control, *IEEE Transactions on Robotics and Automation* 20 (2004) 359–365.
[27] H. Yabuno, H. Matsuda, N. Aoshima, Reachable and stabilizable area of an underactuated manipulator, *IEEE/ASME Transactions on Mechatronics* 10 (2005) 397–403.
[28] A. Tondl, T. Ruijgork, F. Verhulst, R. Nabergoj, *Autoparametric Resonance in Mechanical System*, Cambridge University Press, Cambridge, 2000.
[29] A.H. Nayfeh, B. Balachandran, Modal interaction in dynamical and structural systems, *Applied Mechanics Review* 42 (1989) s175–s201.
[30] R.S. Haxton, A.D.S. Barr, The autoparametric vibration absorber, *Transactions of the ASME Journal of Engineering for Industry* 94 (1972) 119–125.
[31] L. Jun, H. Hongxing, S. Rongying, Saturation-based active absorber for a non-linear plant to a principal external excitation, *Mechanical Systems and Signal Processing* 21 (2007) 1489–1498.
[32] A. Vyas, A. Bajaj, A. Raman, Dynamics of structures with wide-band autoparametric vibration absorbers: theory, *Proceedings of the Royal Society of London Series A* 460 (2004) 11547–11581.
[33] A. Vyas, A. Bajaj, A. Raman, Dynamics of structures with wide-band autoparametric vibration absorbers: experiment, *Proceedings of the Royal Society of London Series A* 460 (2004) 1857–1880.
[34] G. Mustafa, A. Ertas, Dynamics and bifurcations of a coupled column-pendulum oscillator, *Journal of Sound and Vibration* 182 (1995) 393–413.
[35] A.H. Whickens, The dynamics stability of a simplified four-wheel railway vehicle having profiled wheels, *International Journal of Solids and Structures* 1 (1965) 385–406.
[36] A.P. Seyranican, A.A. Mailybaev, *Multiparameter Stability Theory with Mechanical Applications*, World Scientific, Singapore, 2003.
[37] D. Molle, G. Gash, Nonlinear bogie hunting, in: A.H. Wickens (Ed.), Proceedings Seventh IAVSD-Symposium, Lisse, 1982, pp. 455–467.
[38] B. Rogers, D. York, N. Whisman, M. Jone, K. Murray, D. Adams, T. Sulchek, A.C. Minne, Tapping mode atomic force microscopy in liquid with an insulated piezoelectirc microactuator, *Review of Scientific Instruments* 73 (2002) 3242–3244.
[39] H. Yabuno, Analysis and application of nonlinear phenomena (concerned with bifurcation analysis and bifurcation control), *Transactions of the Japan Society of Mechanical Engineers* 73 (2007) 958–965 (in Japanese).
[40] V. Babitsky, Autoresonant mechatronic system, *Mechatronics* 5 (1995) 483–495.
[41] H. Yabuno, S. Saigusa, N. Aoshima, Stabilization of the parametric resonance of a cantilever beam by bifurcation control with a piezo actuator, *Nonlinear Dynamics* 26 (2001) 143–161.
[42] P.L. Kapitza, in: D. Ter Harr (Ed.), Collected Papers by P.L. Kapitza, Vol. 2, Pergamon Press, London, 1965, pp. 714–726.